

COMPUTATIONAL MATERIALS SCIENCE: WHERE THEORY MEETS EXPERIMENTS

Danny E. P. Vanpoucke

Center for Molecular Modeling, Ghent University, Technologiepark 903, 9052 Zwijnaarde,
Belgium

ABSTRACT

In contemporary materials research, we are able to create and manipulate materials at ever smaller scales: the growth of wires with nanoscale dimensions and the deposition of layers with a thickness of only a few atoms are just two examples that have become common practice. At this small scale, quantum mechanical effects become important, and this is where computational materials research comes into play. Using clever approximations, it is possible to simulate systems with a scale relevant for experiments. The resulting theoretical models provide fundamental insights in the underlying physics and chemistry, essential for advancing modern materials research. As a result, the use of computational experiments is rapidly becoming an important tool in materials research both for predictive modeling of new materials and for gaining fundamental insights in the behavior of existing materials. Computer and lab experiments have complementary limitations and strengths; only by combining them can the deepest fundamental secrets of a material be revealed.

In this paper, we discuss the application of computational materials science for nanowires on semiconductor surfaces, ceramic materials and flexible metal-organic frameworks, and how direct comparison can advance insight in the structure and properties of these materials.

COMPUTATIONAL MATERIALS SCIENCE: THIRD LEGG OF A TRIPOD

The physical sciences are generally considered to come in two flavors: experimental and theoretical. However, since the advent of modern computers a third flavor has started to develop: computational. From the 1930's and 40's when computational science started around statistical algorithms (e.g. Monte Carlo simulations),^{1,2} everything moved forward at an ever increasing pace; the 1950's saw the first successful weather prediction based on a computer simulation and the birth of molecular dynamics.^{3,4,5} In the 1960's and 1970's chaos theory received a tremendous boost due to the possibility of using computer programs to calculate fractals and calculate the paths around strange attractors.^{6,7} At the same time, Kohn, Hohenberg and Sham developed density functional theory, which is still one of the most extensively used method in quantum mechanical level materials research.^{8,9} By now, most, if not all, fields in exact science boast a computational flavor. In recent years, also philosophy and sociology saw the introduction of computer simulations, e.g. to study opinion dynamics in populations.^{10,11} From this it is clear that computational science play an ever more prominent role in science.

However, the computational scientist is often the odd duck in the pond, since he/she is neither a unmistakable theoretician (he/she needs to quantify the accuracy of his/her work, she/he does computer "experiments"), nor an obvious experimentalist (you will seldom find one in a lab, and the results he/she presents have an error bar). So what is computational science, more specifically computational materials science (CMS), exactly? Depending on the person asked, you will receive a different reply, and each one equally valid.¹² Some will consider CMS part of the theoretical flavor of materials research, since it deals with models rather than nature itself. While other will consider it as part of the experimental flavor, since they have many common practices regarding their respective 'experiments'. In this paper, I would like to show a third option: CMS as an alternate approach to understanding nature, which at the same time provides

Materials Research

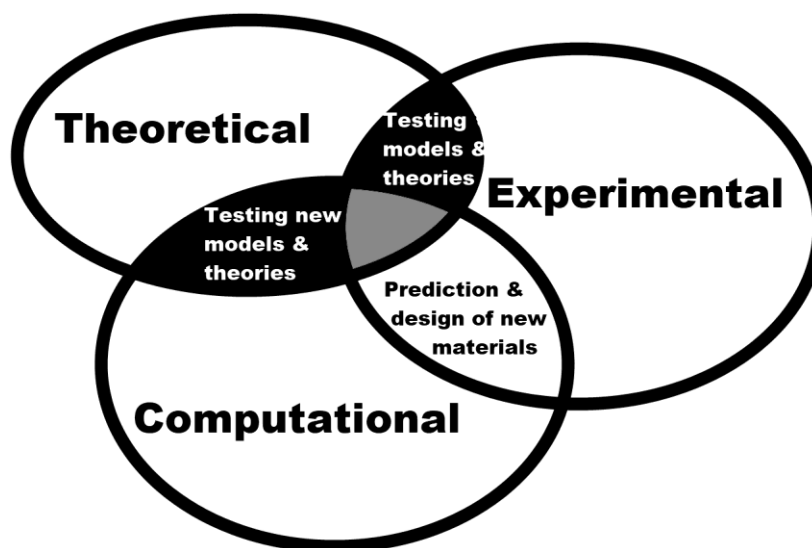


Figure 1: Different flavours of materials research.

the possibility to bridge the often existing gap between theory and experiment: i.e. computational materials science as the third pillar of materials research next to and in between theoretical and experimental materials science.

Each of the three pillars of materials research has the same goal in mind: understanding the nature of materials and consequently, being able to make predictions. Their approaches, however, differ significantly, each with their own strengths and weaknesses.

The experimental scientist studies nature through interaction with it; the materials scientist (chemist or physicist by trade) works with real materials and elicits reactions by mixing materials or probing them in various ways. To do the latter, they make use of (sometimes) very complex machinery, and the analysis of the obtained signals is then generally pulled through one or more models to be boiled down to concepts which are more easily understandable (e.g. from X-ray diffraction (XRD) spectra to lattice parameters). As such the strength of experimental research lies in the direct contact with nature, which in theory frees the researcher from models that may be based on erroneous assumptions. The weakness, however, lies in the machinery and the models required to interpret the signals. In essence, nature will always provide the correct answer, although the scientist might be wrong in his/her understanding of the question he/she is actually asking.

In contrast, the theoretical scientist studies nature from a set of assumptions, which she/he may modify at will or which are rooted in empirical evidence. These assumptions lead to a strongly simplified model of nature, allowing the theoretician to distinguish between main and side issues. Comparison to experimental observations allows the theoretician to discover the fundamental rules of nature. As such, the strength of theoretical work lies in the absolute control over the system of interest (i.e. the theoretician defines all parameters of the model). Its weakness, however, lies in the limited complexity of the models involved, e.g. models assume perfect systems (which is not in line with the average experimental sample) and use a certain level of theory (classical, quantum mechanics,...) which can be a limiting approximation.

The computational scientist draws from both fields; on the one hand he/she uses models, although these models can include much more complexity and are generally speaking no longer analytically solvable. Similar as the theoretician she/he has absolute control over the starting parameters of the model used (i.e. atomic positions, interactions between particles...). On the other hand, just like an experimental scientist he/she will perform multiple simulation experiments to study the response of a system to a modification, and just like the experimental scientist, the computational scientist will(should) calibrate his tools (e.g. convergence testing). As such, the strengths of computational science lies in the fact that much more complex models can be investigated, leading to results which are in closer accordance with nature, albeit with absolute knowledge of the system (e.g. no intuition is required to know where which atom is located). Its weakness on the other hand lies in the limitations of computer resources, and the limitations of the models and algorithms used.

Over the last few decades, experimental materials science has steadily moved to smaller and smaller length scales, making the deposition of layers with a thickness of a single atomic layer, or the growth of wires with nanometer dimensions common practice.^{13,14} Also the manipulation and visualization of individual atoms is no longer a rare feat possible at a single high ranking research facility. At these length scales, quantum effects become increasingly important, and their understanding and accurate prediction a prerequisite for modern device and materials design.

In the same period, computational resources have grown exponentially (Moore's Law¹⁵), leading to desktop computers with the same or even higher performance than top supercomputers two decades earlier. This has had an enormous impact on CMS: Classical(force-field based) molecular dynamics simulations can easily and quickly be run on modern day desktop machines and even small quantum mechanical (QM) level calculations can be run at acceptable speeds.¹² Having access to super computer facilities makes it even possible to tackle systems of several hundreds of atoms at the QM level, making it possible reach sizes which are directly accessible in modern experiments.

With this drive toward nano-scale features in materials science,¹⁶ computational atomic scale modeling has become relevant for real-life device design, since it provides the only means to fully understand and predict properties reigned by QM effects. More importantly, the strengths and weaknesses of experimental and computational techniques are often complementary, as will be seen in the cases below. As such, it is of interest to investigate a problem from both the experimental and computational angle. Furthermore, when direct comparison is possible, the complementarily can provide increased clarity.

In this paper, three examples while be presented where such direct comparison allowed for deeper insights in the systems under study.

DIRECT COMPARISON IN THREE EXAMPLES

Modeling Nanowires On Semiconductor Surfaces

Background And Experimental Research

In the quest for faster and smaller electronics, pushed forward by Moore's Law, Ge is often considered as promising alternative for Si. In recent decades, the formation of atomic scale nanowires (NWs) on Ge surfaces has been observed for many metal/Ge systems. Of these, Pt and Au as metal of choice have received much attention due to the observation of the formation of defect free monatomic wires with lengths up to several hundred nanometers. Although their experimental characterization showed many interesting features, the development of successful models presented difficulties.

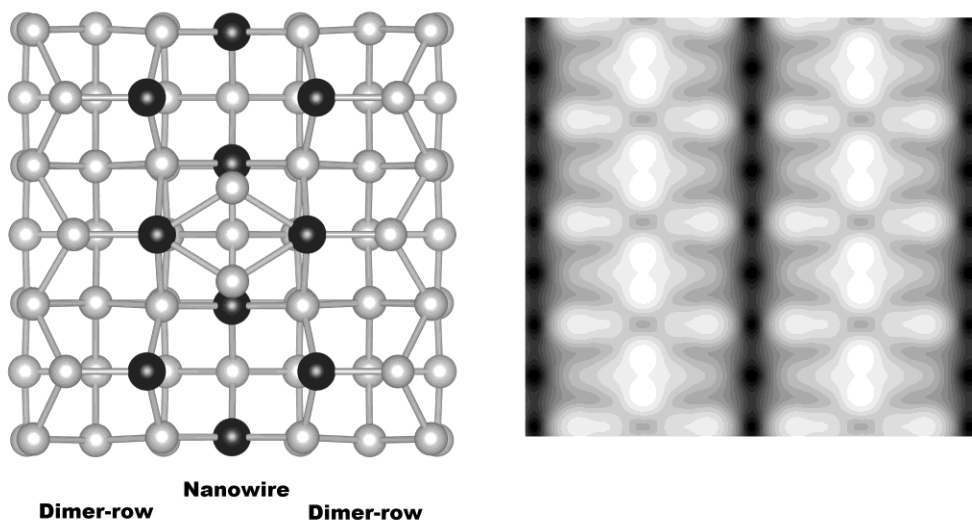


Figure 2: (left) Ball-and-stick representation of the Pt induced nanowire model. Black/grey spheres indicate the positions of the Pt/Ge atoms. (right) Simulated STM image of the Pt induced nanowire model, showing two nanowires.

In 2003, Pt NWs were first observed, in the Zandvliet group, upon deposition of 0.25 monolayer of Pt on a Ge(001) substrate and an annealing sequence at 1050K.¹⁷ The length of the observed NWs was only limited by the size of the underlying terrace, and NWs were observed both as solitary entities and arrays of equally spaced wires. The required anneal temperature, combined with the observation that deposited Pt quickly dives in the Ge substrate, lead to the assumption that the NWs consist of ejected Pt atoms. This assumption was further corroborated by the observation of CO molecules on the NWs, by the same group.^{18,19}

Computational Materials Science: Building Models Towards Experiment

The small scale and perfect periodicity of the NWs made this system an interesting playground for Scanning Tunneling Microscopy (STM) imaging and experiments.^{17,18,19,20,21} At this point, it is important to note that although STM allows one to ‘see’ the atomic positions; it does not tell which atomic species is being observed: STM is chemically insensitive.

The small scale also makes this system well suited for computational study; starting with the attempt to corroborate the experimentally suggested model, since a theoretical model is chemically sensitive by definition.¹⁴

Unfortunately, the experimentally proposed model proved to be energetically unfavorable.^{22,23} Modifications to the substrate model, including additional Pt in the top layer, were able to alleviate this problem, resulting in an energetically favorable Pt NW geometry.^{22,23} However, further attempts to validate this new model by means of comparing simulated and experimental STM images revealed an unforeseen deficiency of the model: the ‘Pt NWs’ were invisible in the simulated STM images. In contrast, a system where the Pt NW chain was replaced by a chain of Ge atoms did clearly present a NW image in the simulated STM images. Further improvements to the surface model were guided by the way the simulated STM image was modified (rather than the energetic stability of the structures) aiming at a more close resemblance to the experimental STM images. This led to the “Pt induced NW model”(figure 2).^{22,23} At the same time and in subsequent years, alternate models were presented, each presenting Ge chains on Pt modified surfaces, and each time simulated STM images were employed as (most) important argument for suggesting the new model.^{24,25} Based on recent

ARPES and RHEPD measurements, however, the Pt induced NW model gained additional experimental support.^{14,26}

A somewhat similar story exists for the Au NWs on Ge system. In 2004, Wang et al.^{27,28} were the first to observe NWs on a Ge(001) surface after the deposition of Au atoms. The Au NWs show similar physical properties as the Pt induced nanowires: equally spaced arrays of perfect NWs only limited by the size of the underlying terrace. A few years later, the groups of Zandvliet and Claesen, independently also observed these Au induced NWs.^{29,30} As for the Pt case, most data presented on this system consists of STM studies. Also initial computational modeling shows promising.^{31,32} Unfortunately, unlike their Pt counterparts, the Au NWs show very few features in room-temperature STM, which is interpreted as a sign that delocalized electrons are present on top of the NWs.^{14,29} This potential access to a (quasi-) one-dimensional metallic state provides a strong boost to experimental interest. Sadly, this also presents a first hint that computational modeling will be non-trivial. Although at the time of writing several models have been proposed, the resulting simulated STM images only show that neither model provides a fully satisfactory representation of the system. However, several experimental features were successfully duplicated in different models.^{14,31}

In conclusion, the combination of computational and experimental results can lead to a more accurate representation of nature observed, but also allows revealing subtly flawed models. Through their combination it is possible to make STM chemically sensitive, which in case of the Pt NWs lead to a more accurate model of the system, and in case of the Au NWs it shows that even though the models are based on sensible intuition they still require further modifications to accurately represent the observed system.

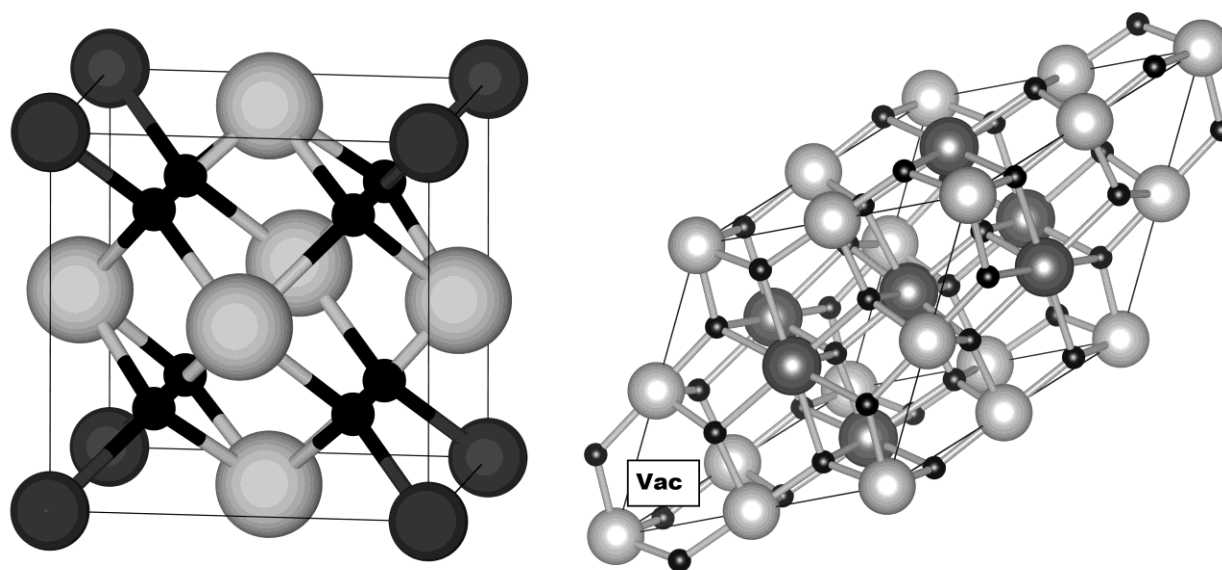


Figure 3: Ball-and-stick representation of the cubic fluorite unit cell (left) and the primitive pyrochlore unit cell (right). Light grey/dark grey spheres show the positions of the Ce/La atoms, while the O positions are indicated by the black spheres. In case of the pyrochlore structure also one of the two vacancies is indicated (Vac).

Tuning Ceramic Materials For Superconductor Applications

Where STM provides an interesting method for direct structural comparison of surfaces, XRD plays this role for bulk materials.

Background And Experimental Research

An interesting example in this regard is the ground state structure of $\text{La}_2\text{Ce}_2\text{O}_7$ (LCO). This material, first synthesized in 1939 by Zintl and Croato,³³ has been studied for the better part of a century, and still its ground state structure remains a point of discussion.^{34,35,36,37,38,39}

Many $\text{A}_2\text{B}_2\text{O}_7$ ternary oxides with lanthanide and transition metal constituents are known to have a pyrochlore crystal structure. As such one could expect the same to be true for LCO. A pyrochlore structure (space group Fd-3m, shown in figure 3) can be derived from the fluorite crystal structure (space group Fm-3m, shown in figure 3) by removing one eighth of the oxygen atoms (Wyckoff 8a site with a B^{IV} cation at the origin), and surrounding this vacancy with four B^{IV} cations (Wyckoff 16c sites), while one oxygen anion (Wyckoff 8b site) is surrounded by four A^{III} cations. The remaining six oxygen anions are each surrounded by two A^{III} and two B^{IV} cations. As such one obtains a structure presenting a clear short range order.

It was, however, also already found by Brisse and Knop in the 1960's that not all $\text{A}_2\text{B}_2\text{O}_7$ ternary oxides present a pyrochlore crystal structure.³⁴ Instead these materials have a defective disordered fluorite structure. In such a structure, the A and B cations are typically randomly distributed over the fluorite cation sub lattice, while one eighth of the oxygen anions are removed (randomly) from the fluorite anion sub lattice. This leads to a structure with no short range order. However, since both the pyrochlore and defective disordered fluorite crystal structures have the same stoichiometry and are both derived from the same fluorite structure, it is clear that they will be very difficult to distinguish in experiments such as XRD or neutron diffraction.

For the $\text{A}_2\text{B}_2\text{O}_7$ ternary oxides it was found that preference for a pyrochlore or a defective disordered fluorite structure is correlated with the ratio of the atomic radii of the A and B cations. The boundary between the two stability regions was empirically determined and it was found that LCO has a cation ratio which is very close to this boundary.^{34,40} As a result, LCO is also of great interest in the study of the order-disorder transition from the pyrochlore to the defective disordered fluorite structure.

Computational Materials Science: Understanding Experimental Spectra

Computational research is perfectly suited for this task, since it allows absolute control over the stoichiometry and the atom positions by the researcher. In addition, it also makes comparison between different configurations possible, irrespective of the fact that these configurations can be synthesized in experiment or even exists in nature as stable structures.

In a two-step approach, different configurations with the same stoichiometry are investigated.³⁸ In the first step, only systems without vacancies are considered. Such configurations could be considered to represent a ternary oxide under a highly oxidizing atmosphere. For these configurations, the defective disordered fluorite structure was found to be favorable over the pyrochlore configuration.³⁸

The inclusion of oxygen vacancies, on the other hand, changes the stability table significantly. This is because in LCO, the oxygen vacancies are shown to present a clear preference for a tetrahedral surrounding containing as much Ce cations as possible.³⁸ Where for the pyrochlore crystal structure 12.5% of all cation tetrahedra consist of only Ce cations, only 6.25% ($=1/2^4$) of the tetrahedra in a disordered fluorite crystal structure contain four Ce cations. Since in an $\text{A}_2\text{B}_2\text{O}_7$ ternary oxide 12.5% of all cation tetrahedra contain an oxygen vacancy, only

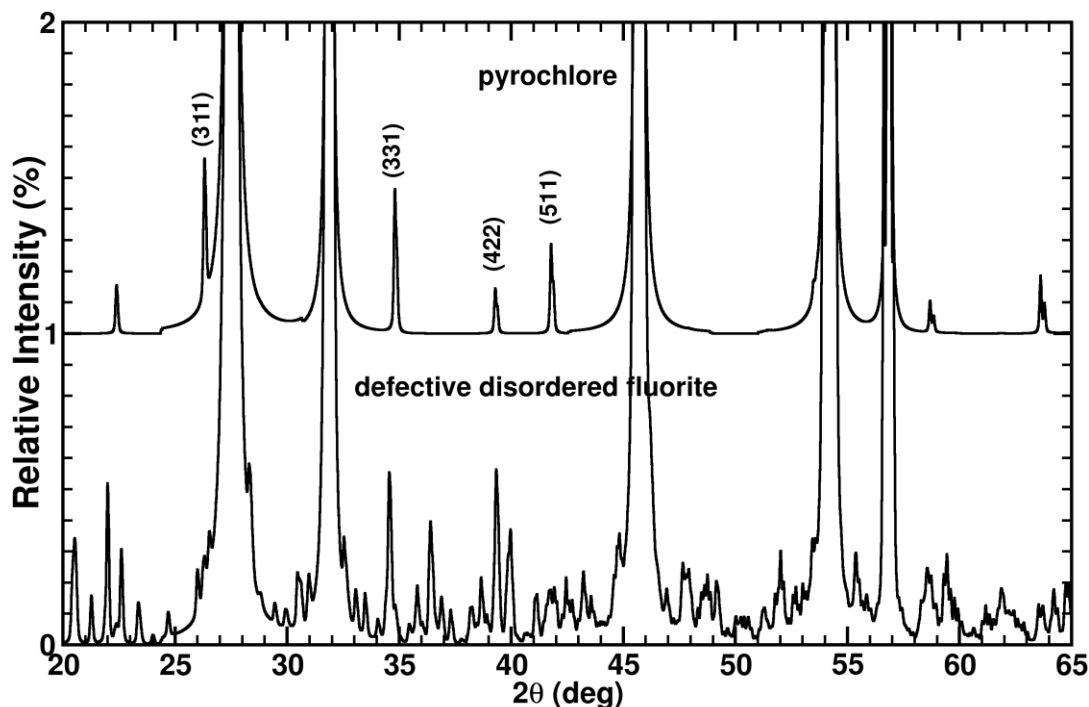


Figure 4: Comparison of the simulated XRD spectra for the pyrochlore (top, shifted by 1%) and defective disordered fluorite (bottom) structures. Prototypical pyrochlore reflections are indicated. Note the intensity scale.

the pyrochlore structure will be able to provide full Ce tetrahedra all vacancies, while in the disordered fluorite at least half of the oxygen vacancies will have a less than optimal tetrahedral surrounding.

Because the formation enthalpies are functional dependent, and density functional theory calculations do not consider either temperature or pressure, further approaches are required to compare to experiment. At this point, we turn our attention to XRD. Although lattice parameters and atomic positions are, in experiment, routinely derived from XRD patterns, the similarity between the pyrochlore and defective disordered fluorite structure make this an unsuitable path of inquiry. Instead, the inverse path, simulating an XRD pattern starting from the computational model structure, is better suited since in this case the origin of the XRD reflections is explicitly known. As such, comparison of simulated and experimental XRD patterns is the route to follow. In case of the LCO system, this shows that all high intensity reflections are present for both models, although their relative intensity is slightly better in case of the pyrochlore model (figure 4). More importantly, the simulated XRD patterns explain why the prototypical pyrochlore reflections might not be observed in experiment: their relative intensity is too small (<1%) to be distinguished from background noise in standard XRD measurements.^{38,39}

Flexibility And Spin Configurations In Metal-Organic Frameworks

As was shown in the previous two cases, computational methods provide many diverse ways to investigate atomic scale systems and compare them to experiments. The control over the model allows the computational researcher to simulate systems that are hard or impossible to synthesize.

Background And Experimental Research

In this example, we will look at a class of complex systems: breathing metal-organic frameworks (MOFs).^{41,42,43,44,45} A MOF is said to show breathing behavior if a reversible structural phase transition exists which is accompanied by a significant change in volume (~50%). During such a phase transition the topology of the system is retained, and the transition is triggered by an external stimulus such as temperature, gas sorption or applied pressure.

In case of the MIL-47(V) MOF,^{43,44,45} breathing only occurs under the influence of an external pressure. More interestingly, in experiments, this transition is not sharply defined at one specific pressure, but occurs over a range of pressures, leading to an s-shaped V(P) curve for a sample. The origin of this behavior is unknown.⁴³

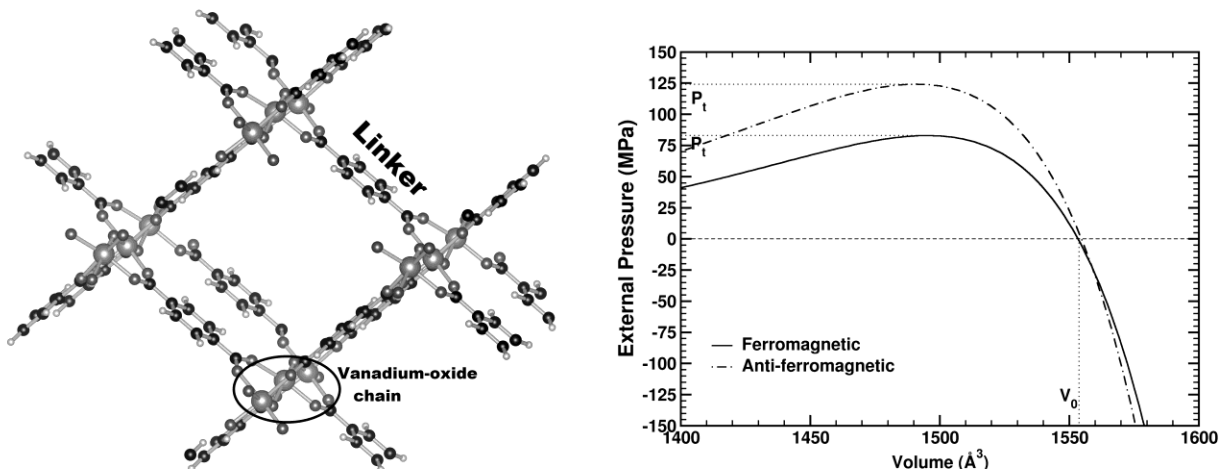


Figure 5: Ball-and-stick representation of the MIL-47(V) MOF (left). Calculated P(V) curves for the ferromagnetic and antiferromagnetic configurations of the MIL-47(V) MOF (right). The equilibrium volume V_0 , and transition pressures P_t are indicated.

Computational Materials Science: Understanding And Predicting Experiment

Computational treatment of the material is complicated by the fact that each vanadium atom contains one unpaired electron, resulting in 2^n configurations for a cell containing n vanadium atoms. In case of the MIL-47(V) MOF, it was shown that the inter-chain coupling between the vanadium atoms is negligible and intra-chain couplings govern the system making it quasi-one-dimensional.⁴⁵ Where the spin configuration does not play an important role in the mechanical properties of most periodic bulk systems, it does in this case: The bulk modulus reduces with 25% going from 8 GPa for anti-ferromagnetic chains to 6 GPa for ferromagnetic chains. In contrast, the structural parameters of the different spin configurations are nearly indistinguishable.⁴⁵

Using the calculated equilibrium volume, energy, bulk modulus and pressure derivative of the bulk modulus, it is possible to calculate a P(V) curve for the different spin configurations of the MIL-47(V). As is shown in figure 5, increasing the pressure reduces the volume up to a certain point. At this transition pressure P_t , the volume will present a sudden jump (structural phase transition). The pressure and volume at which this transition occurs was shown to depend on the spin configuration. Furthermore, mixed systems, containing both anti-ferromagnetic and ferromagnetic chains, show transition pressures which are a weighted average of the transition

pressures of the purely ferromagnetic and purely anti-ferromagnetic systems. Since the transition pressure of these pure systems coincide with the experimentally observed boundaries of the transition pressure in Hg-intrusion experiments,⁴³ this provides us with an explanation of the experimental observation: The experimental sample contained grains with varying ratios of anti-ferromagnetic/ferromagnetic chains leading to a range of transition pressures, starting at that of a fully ferromagnetic system (82 MPa), up to those of a fully anti-ferromagnetic system (124 MPa).⁴⁵

CONCLUSIONS

In this work we have presented and discussed the merits of computational materials science, and the role it can play in a combined research approach within materials science. By using the complementary strengths of computational and experimental methods, it is possible to make STM chemically sensitive and provide a more powerful validation tool for models of surface structure reconstructions. In case of metal nanowires on the Ge(001) surface this approach has been shown to be invaluable with regard to the modeling effort.

Also the modeling of bulk materials can benefit from direct comparison between computational and experimental data. Simulated XRD data can provide important insights in experimental XRD spectra of systems where multiple models are difficult to distinguish. In case of the $\text{La}_2\text{Ce}_2\text{O}_7$ system it showed that prototypical pyrochlore reflections might be too small for experimental observation, which may result in an erroneous choice of model for this system.

Finally, computational methods give access to parameters that are hard or impossible to control in experiments, allowing one to discover important aspects influencing macroscopic properties. In case of the MIL-47(V) breathing MOF, the range in transition pressures could be related to varying spin configurations of the sample grains.

ACKNOWLEDGEMENTS

The author is a postdoctoral researcher funded by the Foundation of Scientific Research-Flanders (FWO) (project no. 12S3415N). For the computational resources (Stevin Supercomputer Infrastructure) and services used, related to this work, he acknowledges the VSC (Flemish Supercomputer Center), funded by Ghent University, the Hercules Foundation and the Flemish Government – department EWI.

APPENDIX: COMPUTATIONAL METHODS

In the examples presented in this work, all *ab-initio* calculations are performed using the Vienna Ab-initio Simulation Package (VASP).⁴⁶⁻⁴⁸ Because of the size of the systems, we make use of Density Functional Theory (DFT) combined with the Projector Augmented Wave (PAW) method. All calculations make use of periodic boundary conditions, and for more detailed information on the specific setting regarding the kinetic energy cutoff, k-points set and the structural optimization settings used we refer to references 14, 22, 23 for the STM/nanowires example, reference 38 for the XRD/ $\text{La}_2\text{Ce}_2\text{O}_7$ example and reference 45 for the transition pressure/MOF example.

Post-processing of the *ab-initio* data to obtain STM images was done using the HIVE-STM code,⁴⁹ while XRD spectra were generated using the XRD-tool of the ICSD crystallographic database.⁵⁰ For the equation of state-fitting and generation of P(V) curves and calculation of transition pressures an in-house developed tool-box was used.⁵¹

REFERENCES AND FOOTNOTES

- ¹ Ulam, S., Richtmyer, R. D., & von Neumann, J. (1947). Statistical methods in neutron diffusion. *Los Alamos Scientific Laboratory report LAMS-551*.
- ² Metropolis, N., & Ulam, S. (1949). The Monte Carlo method. *Journal of the American Statistical Association, Volume 44*, 335–341.
- ³ Charney, J., Fjørtoft, R., & von Neumann, J. (1950). Numerical Integration of the Barotropic Vorticity Equation. *Tellus, Volume 2(4)*.
- ⁴ Alder, B. J., & Wainwright, T. E. (1959). "Studies in Molecular Dynamics. I. General Method". *The Journal of Chemical Physics, Volume 31*, 459-466.
- ⁵ Rahman, A. (1964). Correlations in the Motion of Atoms in Liquid Argon. *Physical Review, Volume 136*, A405–A411.
- ⁶ Lorenz, E. N. (1963). Deterministic Nonperiodic Flow. *Journal of the Atmospheric Sciences, Volume 20*, 130–141.
- ⁷ Mandelbrot, B. B. 1983. *The Fractal Geometry of Nature*. San Francisco: W.H. Freeman. ISBN 0-7167-1186-9.
- ⁸ Hohenberg, P. & Kohn, W.(1964). Inhomogeneous Electron Gas. *Physical Review, Volume 136*, B864–B871.
- ⁹ Kohn, W., & Sham, L.J. (1965). Self-Consistent Equations Including Exchange and Correlation Effects. *Physical Review, Volume 140*, A1133–A1138.
- ¹⁰ Hegselmann, R. & Krause, U. (2006). Truth and cognitive division of labor: first steps towards a computer aided social epistemology. *Journal of Artificial Societies and Social Simulation, Volume 9*, 3.
- ¹¹ Wenmackers, S., Vanpoucke, D. E. P., & Douven, I. (2014), Rationality: a social-epistemology perspective. *Frontier in Psychology, Volume 5*, 581.
- ¹² Ercolessi, F. A molecular dynamics primer. Spring College in Computational Physics, ICTP, Trieste, June 1997. <http://www.sissa.it/furio/>
- ¹³ Barth, J.V., Constantini, G. & Kern, K. (2005), Engineering atomic and molecular nanostructures at surfaces. *Nature, Volume 437*, 671-679, and references therein.
- ¹⁴ Vanpoucke, D.E.P. (2014), Modeling 1D structures on semiconductor surfaces: Synergy of theory and experiment. *Journal of Physics : Condensed Matter, Volume 26*, 133001.
- ¹⁵ Moore, G.E. (1965). Cramming more components onto integrated circuits, *Electronics, Volume 38*, 8.
- ¹⁶ Xbit, Intel Outlines Process Technology Roadmap, http://www.xbitlabs.com/news/cpu/display/20090822094141_Intel_Outlines_Process_Technology_Roadmap.html (2009-08-22).
- ¹⁷ Gurlu, O., Adam, O. A. O., Zandvliet, H. J. W., & Poelsema, B. (2003). Self-organized, one-dimensional Pt nanowires on Ge(001). *Applied Physics Letters, Volume 83*, 4610-4612.
- ¹⁸ Oncel, N., van Beek, W. J., Huijben, J., Poelsema, B., & Zandvliet, H. J. W. (2006). Diffusion and binding of CO on Pt nanowires. *Surface Science, Volume 600*, 4690-4693.
- ¹⁹ Kockmann, D., Poelsema, B., & Zandvliet, H. J. W. (2008). Remarkably long-ranged repulsive interaction between adsorbed CO molecules on Pt modified Ge(001). *Physical Review B, Volume 78*, 245421.
- ²⁰ Zandvliet, H. J. W. , van Houselt, A., & Poelsema, B. (2009). Self-lacing atom chains. *Journal of Physics: Condensed Matter, Volume 21*, 474207.
- ²¹ Heimbuch, R., Wu, H., Kumar, A., Poelsema, B., Schon, P., Vasco, G.J. & Zandvliet, H. J. W. (2012). Variable-temperature study of the transport through a single octanethiol molecule. *Physical Review B, Volume 86*, 075456.
- ²² Vanpoucke, D. E. P. & Brocks, G. (2008). Formation of Pt-induced Ge atomic nanowires on Pt/Ge(001): A density functional theory study. *Physical Review B, Volume 77*, 241308(R).

- ²³ Vanpoucke, D. E. P. & Brocks, G. (2010). Pt-induced nanowires on Ge(001): A density functional theory study. *Physical Review B, Volume 81*, 085410.
- ²⁴ A. A. Stekolnikov, A.A., Furthmuller, J., & Bechstedt, F. (2008). Pt-induced nanowires on Ge(001): Ab initio study. *Physical Review B, Volume 78*, 155434.
- ²⁵ Tsay, S.-F. (2012). Pt-chain induced formation of Ge nanowires on the Ge(001) surface. *Surface Science, Volume 606*, 1405-1411.
- ²⁶ Mochizuki, I., Fukaya, Y., Kawasuso, A., Yaji, K., Harasawa, A., Matsuda, I., Wada, K., & Hyodo, T. (2012). Atomic configuration and phase transition of Pt-induced nanowires on a Ge(001) surface studied using scanning tunneling microscopy, reflection high-energy positron diffraction, and angle-resolved photoemission spectroscopy. *Physical Review B, Volume 85*, 245438.
- ²⁷ Wang, J., Li, M., & Altman, E. I. (2004). Scanning tunneling microscopy study of self-organized Au atomic chain growth on Ge(001). *Physical Review B, Volume 70*, 233312.
- ²⁸ Wang, J., Li, M., & Altman, E. I. (2005). Scanning tunneling microscopy study of Au growth on Ge(001): Bulk migration, self-organisation, and clustering. *Surface Science, Volume 596*, 126-143.
- ²⁹ Schafer, J., Blumenstein, C., Meyer, S., Wisniewski, M., & Claessen, R. (2008). New Model System for a One-Dimensional Electron Liquid: Self-Organized Atomic Gold Chains on Ge(001). *Physical Review Letters, Volume 101*, 236802.
- ³⁰ van Houselt, A., Fischer, M., Poelsema, B., & Zandvliet, H. J. W. (2008). Giant missing row reconstruction of Au on Ge(001). *Physical Review B, Volume 78*, 233410.
- ³¹ Sauer, S., Fuchs, F., Bechstedt, F., Blumenstein, C., & Schafer, J. (2010). First-principles studies of Au-induced nanowires on Ge(001). *Physical Review B, Volume 81*, 075412.
- ³² Lopez-Moreno, S., Romero, A. H., Munoz, A., & Schwingenschlogl, U. (2010). First-principles description of atomic gold chains on Ge(001). *Physical Review B, Volume 81*, 041415.
- ³³ Zintl, E. & Croatto, U. (1939). Fluoritgitter mit leeren Anionenplätzen. *Zeitschrift für Anorganische und Allgemeine Chemie, Volume 242*, 79-86.
- ³⁴ Brisse, F., & Knop, O. (1967). Pyrochlores. II. An investigation of $\text{La}_2\text{Ce}_2\text{O}_7$ by neutron diffraction. *Canadian Journal of Chemistry, Volume 45*, 609-614.
- ³⁵ Yamamura, H., Nishino, H., Kakinuma, K., & Nomura, K. (2003). Crystal phase and electrical conductivity in the pyrochlore-type composition systems, $\text{Ln}_2\text{Ce}_2\text{O}_7$ ($\text{Ln} = \text{La}, \text{Nd}, \text{Sm}, \text{Eu}, \text{Gd}, \text{Y}$ and Yb). *Journal of the Ceramic Society of Japan, Volume 111*, 902-906.
- ³⁶ Bae, J. S., Choo, W. K. & Lee, C. H. (2004). The crystal structure of ionic conductor $\text{La}_x\text{Ce}_{1-x}\text{O}_{2-x/2}$. *Journal of the European Ceramics Society, Volume 24*, 1291-1294.
- ³⁷ Ryan, K. M., McGrath, J. P., Farrell, R. A., O'Neill, W. M., Barnes, C. J., & Morris, M. A. (2003). Measurements of the lattice constant of ceria when doped with lanthana and praseodymia - the possibility of local defect ordering and the observation of extensive phase separation. *Journal of Physics : Condensed Matter, Volume 15*, L49-L58.
- ³⁸ Vanpoucke, D.E.P., Bultinck, P., Cottenier, S., Van Speybroeck, V. & Van Driessche, I. (2011). Density functional theory study of $\text{La}_2\text{Ce}_2\text{O}_7$: Disordered fluorite versus pyrochlore structure. *Physical Review B, Volume 84*, 054110.
- ³⁹ Reynolds, E., Blanchard, P. E. R., Zhou, Q., Kennedy, B.J., Zhang, Z.M., & Jang, L.Y. (2012). Structural and spectroscopic studies of $\text{La}_2\text{Ce}_2\text{O}_7$: Disordered fluorite versus pyrochlore structure. *Physical Review B, Volume 85*, 132101.
- ⁴⁰ Minervini, L., Grimes, R. W., & Sickafus, K. E. (2000). Disorder in Pyrochlore Oxides. *Journal of the American Ceramics Society, Volume 83*, 1873-1878.

- ⁴¹ Llewellyn, P. L., Bourrelly, S., Serre, C., Filinchuk, Y., & Férey, G. (2006). How Hydration Drastically Improves Adsorption Selectivity for CO₂ over CH₄ in the Flexible Chromium Terephthalate MIL-53. *Angewandte Chemie, International Edition, Volume 45*, 7751–7754.
- ⁴² Serre, C., Bourrelly, S., Vimont, A., Ramsahye, N. A., Maurin, G., Llewellyn, P. L., Daturi, M., Filinchuk, Y., Leynaud, O., Barnes, P., & Férey, G. (2007). An Explanation for the Very Large Breathing Effect of a Metal–Organic Framework during CO₂ Adsorption. *Advanced Materials, Volume 19*, 2246–2251.
- ⁴³ Yot, P. G., Ma, Q., Haines, J., Yang, Q., Ghoufi, A., Devic, T., Serre, C., Dmitriev, V., Férey, G., Zhong, C., & Maurin, G. (2012). Large breathing of the MOF MIL-47(V^{IV}) under mechanical pressure: a joint experimental-modelling exploration. *Chemical Science, Volume 3*, 1100–1104.
- ⁴⁴ Barthelet, K., Marrot, J., Riou, D., & Férey, G. (2002). A Breathing Hybrid Organic–Inorganic Solid with Very Large Pores and High Magnetic Characteristics. *Angewandte Chemie, International Edition, Volume 41*, 281–284.
- ⁴⁵ Vanpoucke, D.E.P., Jaeken, J.W., De Baerdemacker, S., Lejaeghere, K. & Van Speybroeck, V. (2014). Quasi-1D physics in metal-organic frameworks: MIL-47(V) from first principles. *Beilstein Journal of Nanotechnology, Volume 5*, 1738–1748.
- ⁴⁶ Kresse, G., & Joubert, D. (1999). From ultrasoft pseudopotentials to the projector augmented-wave method. *Physical Review B, Volume 59*, 1758–1775.
- ⁴⁷ Kresse, G., & Hafner, J. (1993). Ab initio molecular dynamics for liquid metals. *Physical Review B, Volume 47*, 558–561.
- ⁴⁸ Kresse, G., & Furthmüller, J. (1996). Efficient iterative schemes for ab initio total-energy calculations using a plane-wave basis set. *Physical Review B, Volume 54*, 11169–11186.
- ⁴⁹ Vanpoucke, D.E.P. HIVE STM. <http://dannyvanpoucke.be/hive-stm-en/> (accessed April 7, 2015).
- ⁵⁰ Bergerho, G., & Brown, I. D. (1987). In *Crystallographic Databases*, edited by Allen, F.H., Bergerho, G., & Sievers, R. (International Union of Crystallography, Chester, 1987), Volume 77.
- ⁵¹ Vanpoucke, D.E.P. HIVE 3.x STM. <http://dannyvanpoucke.be/computational-science-en/> (accessed April 7, 2015).